

Article

Use of a Highly Specialized Biocatalyst to Produce Lactate or Biohydrogen and Butyrate from Agro-Industrial Resources in a Dual-Phase Dark Fermentation

Octavio García-Depraect ^{1,2,*}  and Elizabeth León-Becerril ^{3,*} ¹ Institute of Sustainable Processes, University of Valladolid, Dr. Mergelina, s/n., 47011 Valladolid, Spain² Department of Chemical Engineering and Environmental Technology, University of Valladolid, Dr. Mergelina, s/n., 47011 Valladolid, Spain³ Centro de Investigación y Asistencia en Tecnología y Diseño del Estado de Jalisco, Department of Environmental Technology, A.C., Av. Normalistas 800, Colinas de la Normal, Guadalajara 44270, Jalisco, Mexico

* Correspondence: octavio.garcia@uva.es (O.G.-D.); eleon@ciatej.mx (E.L.-B.)

Abstract: This study aimed at investigating the feasibility of using a highly specialized bacterial inoculum harboring lactic acid bacteria (LAB) and lactate-oxidizing, hydrogen-producing bacteria (LO-HPB) to produce either lactate or biohydrogen and butyrate from several agro-industrial resources via dual-phase dark fermentation. The feedstocks were fruit–vegetable waste, cheese whey, coffee wastewater, tequila vinasse, and maize processing wastewater, and were tested in both mono- and co-fermentation. The results obtained indicated that the biocatalyst used was able to perform a dual-phase lactate fermentation, producing high lactate (13.1–36.4 g/L), biohydrogen (0.2–7.5 NL H₂/L_{feedstock}, equivalent to 0.3–1.7 mol H₂/mol hexose), and butyrate (3.3–13.9 g/L) with all the tested feedstocks. A series of self-fermentation tests were also performed with crude cheese whey and fruit–vegetable waste for comparison purposes. Compared to inoculum-aided fermentations, the self-fermentation exhibited a reduced bioconversion efficiency. Short-length 16S rRNA gene sequencing analysis showed that LO-HPB was the dominant microbial group (86.0%) in the biocatalyst, followed by acetic acid bacteria (5.8%) and LAB (5.7%). As expected, the molecular analysis also showed significant differences in the microbial community structure of the biocatalyst and those that evolved from self-fermentation. Besides lactate fermentation and oxidation, the biocatalyst also assisted the bi-phasic lactate fermentation via oxygen consumption, and apparently, via substrate hydrolysis. Overall, this study can lay the foundation for robust inoculum development, which is of special significance in the field of dark fermentation, and proposes an innovative bioprocess for agro-industrial valorization through a trade-off approach, tailoring the metabolic pathway to the target product(s).

Keywords: biohydrogen; biorefinery; dark fermentation; inoculum development; organic acids; organic waste



Citation: García-Depraect, O.; León-Becerril, E. Use of a Highly Specialized Biocatalyst to Produce Lactate or Biohydrogen and Butyrate from Agro-Industrial Resources in a Dual-Phase Dark Fermentation. *Fermentation* **2023**, *9*, 787. <https://doi.org/10.3390/fermentation9090787>

Academic Editor: Yuriy Litt

Received: 29 July 2023

Revised: 21 August 2023

Accepted: 22 August 2023

Published: 25 August 2023



Copyright: © 2023 by the authors. Licensee MDPI, Basel, Switzerland. This article is an open access article distributed under the terms and conditions of the Creative Commons Attribution (CC BY) license (<https://creativecommons.org/licenses/by/4.0/>).

1. Introduction

Dark fermentation (DF) is a promising platform to produce biogenic renewable hydrogen and organic acids within a biorefinery approach. Hydrogen can be used either as feedstock in diverse industrial processes or as an energy carrier due to its high energy content (141.9 MJ/kg), while organic acids are value-added products that can be further utilized as building blocks [1–3]. Metabolically, DF involves the hydrolysis and acidogenesis of fermentable organics, leading to the production of hydrogen and organic acids by the action of hydrolytic and acidogenic bacteria under anoxic and dark conditions. The DF process can be driven using a bacterial inoculum or by the microorganisms already present in a given feedstock, the so-called self-fermentation or natural fermentation. DF

is seen as the most advantageous way to produce biogenic hydrogen today, as it does not need light energy, can be fed with several organic wastes/wastewaters, and can sustain higher hydrogen production rates than biophotolysis, photofermentation, and microbial electrolysis cells [4]. Under DF conditions, approximately one-third of the total energy available in the fermentable organic content of biomass can be theoretically recovered as hydrogen, but in practice, hydrogen yields are typically lower [1]. Bacteria belonging to the genera *Clostridium*, *Bacillus*, *Enterobacter*, *Citrobacter*, and *Klebsiella* are some fermentative hydrogen producers [5]. Reactor design, biomass pretreatment, microbial immobilization, additives supply, metabolic engineering, bioaugmentation, and microbial enrichment have been some strategies used to enhance the performance of the DF process [6]. However, the major bottlenecks of DF still include low hydrogen yield, process instability, the production of inhibitory by-products, the presence of hydrogen-consuming bacteria, and substrate complexity [6]. Furthermore, there is currently a lack of industrial, robust biocatalysts, which are a keystone for the development and deployment of the envisioned large-scale dark fermentative systems [7]. The ideal inoculum must be robust enough not only against non-sterile conditions and unforeseen operational problems (e.g., sudden acidification, organic overloading, famine conditions, etc.) but also against the presence of undesirable microorganisms including the latent invasion of indigenous microflora present in the feedstock, which may compete for the substrate and/or consume the hydrogen produced [1,6,7]. Additionally, ideal DF biocatalysts must also possess a flexible and diverse metabolic machinery that allows one to efficiently produce hydrogen and organic acids as by-products from complex substrates such as agro-industrial residues [8]. In this regard, because they are frequently highly biodegradable, abundant, and cheap, agro-industrial residues are rather potential renewable resources for DF-based valorization processes [9].

Typically, hydrogen production via DF occurs through the fermentation of carbohydrates via acetic-type and butyric-type pathways. However, over the last years, the production of hydrogen through syntrophic interactions between lactic acid bacteria (LAB) and lactate-oxidizing, hydrogen-producing bacteria (LO-HPB) has gained increasing scientific attention [8,10,11]. Several hydrogen-producing biocatalysts have been characterized to be accompanied by LAB [10]. The effect of LAB in DF is still ambiguous, as they are often reported to lead to high hydrogen production, but in other cases, they are related to a poor one due to substrate competition, the excretion of bacteriocins, and the acidification of the broth [10,11]. The root reason why sometimes LAB act as helpers for hydrogen production whereas on other occasions they act as antagonist remains poorly understood. When LAB play a positive role in DF, they coexist with LO-HPB by performing, in simple terms, two-step lactate fermentation. In this vein, LAB can perform the first lactate fermentation transforming fermentable carbohydrates into lactate or lactate and acetate, while LO-HPB can assimilate such lactate together with acetate to produce hydrogen and butyrate [12,13]. The use of LAB in DF systems is still minimized despite their different auxiliary activities, which include pH regulation, substrate hydrolysis, biomass retention, oxygen depletion, and hydrogen production [10]. Besides these advantages, exploiting the syntrophic associations between LAB and LO-HPB via dual-phase fermentation not only allows the production of hydrogen and butyrate but it can also produce lactate in an acidogenic trade-off approach [14]. Butyrate can be used as an animal and human food additive, solvent, flavoring agent, chemical intermediate, and other applications, while lactate is a commodity that can be employed in the food, pharmaceutical, textile, detergent, leather, and plastic industries [15,16]. The importance of promoting a robust biocatalyst performing lactate-driven DF becomes evident when one takes into account that a number of agro-industrial residues are suitable to support the growth of LAB, including tequila vinasse (TV) and maize processing wastewater (MPW) [17], fruit and vegetable waste (FVW) and cheese whey (CCW) [18], brewery wastewater [19], ethanol fermentation residues [20], ensiled wastes [21], and food waste [22], among others. Moreover, it should be noted that in DF systems, it is quite challenging to wash out LAB either via pretreatment of the feedstock/inoculum due to economic restrictions, or via the modula-

tion of process/environmental conditions (e.g., temperature, pH, hydraulic retention time, and organic loading rate) due to LAB can generally grow well under those conditions conducive for DF.

Hence, this study proposes for the first time the use of a highly specialized biocatalyst, which is mainly composed of LAB and LO-HPB to produce valuable lactate or hydrogen and butyrate from several agro-industrial resources (i.e., TV, CCW, FVW, MPW, and coffee wastewater (CWW)) in both mono- and co-fermentation approaches. The capacity of the biocatalyst to provide a suitable reducing environment by removing residual oxygen was also assessed. Additionally, self-fermentation tests were also run for the sake of comparison. Finally, the microbial community structure of the biocatalyst and the indigenous microflora that evolved during the self-fermentation of FVW and CCW was analyzed. The significance and originality of this study are that it proposes a biotechnological process based on a dual-phase lactate fermentation for the valorization of agro-industrial wastes and provides evidence that it is possible to tailor DF by using a suitable biocatalyst with an improved potential metabolic activity.

2. Materials and Methods

2.1. Inoculum

The source of the biocatalyst utilized was digestate obtained from an anaerobic digester treating food waste, which was pretreated by applying alternating cycles of transient and moderate microaeration and heat shock (90 °C for 20 min). The inoculum was grown on glucose for 2 months to enrich LAB and LO-HPB [14]. After such a step, it was preserved under refrigeration (4 °C) until use [23]. To activate the dormant bacteria, a pre-fermentation step was carried out in a 1-L gas-tight glass bottle with a working volume of 0.5 L for 24 h using glucose (10 g/L) as the sole carbon source and a mineral salt medium containing (in g/L) NH_4Cl , 2.4; K_2HPO_4 , 2.4; $\text{MgSO}_4 \cdot 7\text{H}_2\text{O}$, 1.5; KH_2PO_4 , 0.6; CaCl_2 , 0.11; and $\text{FeSO}_4 \cdot 7\text{H}_2\text{O}$, 0.05 [14,24].

2.2. Feedstocks

Different agro-industrial resources were tested in mono- and co-fermentation systems. FVW, CCW, CWW, and TV were examined through a mono-fermentation approach, whereas blends of TV and MPW (80/20 *w/w*), CCW and FVW (66/34 *w/w*), and TV and CCW (80/20 *w/w*) were tested through a co-fermentation one. Overripe fruit and vegetables, i.e., banana, papaya, mango, watermelon, pineapple, tomato, potato, and carrot, were collected from a local market. FVW was prepared by processing a mixture consisting of 900 g of each fruit/vegetable, including the peel and the pulp. The mixture was blended with 800 mL of tap water and sieved through a 4-mm stainless steel mesh. Likewise, CCW was collected from a local cheese manufacturing plant using cow milk. CCW was passed through a filter with a pore diameter of 8 µm to remove lipids and suspended solids. CWW was kindly provided by a coffee processing factory located in Veracruz, Mexico. CWW was composed of wastewater derived from the fermentation (20% *v/v*) and demucilization (80% *v/v*) steps of Arabica coffee beans. The wastewater from demucilization was filtered through a 1-mm stainless steel mesh before use. MPW was provided by a local maize processing industry making tortillas. Finally, TV was collected from a tequila factory located in Tequila, Jalisco, Mexico. All the feedstocks used were stored in plastic containers at 4 °C. Their physicochemical features are given in Table 1.

Table 1. Physicochemical characterization of feedstocks.

Parameter	TV	FVW	CWW	CCW	TV-MPW	FVW-CCW	TV-CCW
Total COD (g/L)	72.3 ± 0.1	100.2 ± 0.3	42.6 ± 0.6	89.4 ± 0.3	66.5 ± 0.1	110.3 ± 0.4	72.6 ± 3.2
Soluble COD (g/L)	58.6 ± 0.3	70.7 ± 0.1	26.9 ± 0.1	61.6 ± 0.0	42.9 ± 0.3	65.7 ± 0.1	56.9 ± 1.2
BOD (g/L)	32.1 ± 1.0	62.9 ± 1.7	17.1 ± 1.2	55.5 ± 0.4	32.9 ± 1.2	61.9 ± 5.6	39.1 ± 4.5
TOC (g/L)	21.7 ± 0.1	24.5 ± 0.2	11.0 ± 0.1	20.5 ± 0.1	21.7 ± 0.1	28.7 ± 0.1	22.2 ± 0.5
Total nitrogen (mg/L)	201.0 ± 1.4	850.0 ± 0.0	26.5 ± 0.7	1405.0 ± 7.1	225.0 ± 7.1	870.0 ± 14.1	515.0 ± 7.1
Total phosphorous (mg/L)	465.0 ± 2.8	490.5 ± 5.0	169.5 ± 0.7	573.5 ± 3.5	354.5 ± 3.5	599.5 ± 0.7	467.5 ± 24.8
TS (g/L)	52.2 ± 1.1	102.2 ± 0.2	19.9 ± 0.2	66.3 ± 2.1	44.0 ± 0.1	78.5 ± 3.2	52.6 ± 0.8
TVS (g/L)	48.5 ± 1.0	97.6 ± 0.5	18.5 ± 0.3	61.1 ± 2.1	40.1 ± 0.2	73.3 ± 3.0	48.5 ± 0.6
TDS (g/L)	27.5 ± 3.0	69.4 ± 3.1	9.7 ± 0.9	50.9 ± 2.2	23.1 ± 4.6	51.9 ± 9.0	24.8 ± 2.8
TSS (g/L)	24.7 ± 2.3	32.7 ± 3.3	10.5 ± 0.8	15.4 ± 0.2	20.9 ± 4.5	26.6 ± 6.4	27.8 ± 2.1
pH	3.6 ± 0.0	4.2 ± 0.1	3.7 ± 0.0	4.2 ± 0.1	3.9 ± 0.0	4.2 ± 0.0	3.8 ± 0.1
Total alkalinity (mg CaCO ₃ eq./L)	-	-	-	-	670.0 ± 1.3	-	-
Total acidity (g CaCO ₃ eq./L)	4.9 ± 0.0	1.7 ± 0.0	2.4 ± 0.0	2.3 ± 0.0	3.6 ± 0.3	2.6 ± 0.0	5.4 ± 0.2
Reducing sugars (g/L)	12.7 ± 0.4	35.3 ± 0.5	2.9 ± 0.0	34.4 ± 0.0	11.6 ± 0.9	31.3 ± 0.2	16.5 ± 0.1
Total carbohydrates (g/L)	25.2 ± 3.2	63.0 ± 0.7	2.9 ± 0.4	44.8 ± 0.4	19.3 ± 1.2	44.0 ± 2.2	24.5 ± 0.6
Sulphate (g/L)	1.0 ± 0.0	0.1 ± 0.0	1.0 ± 0.0	0.7 ± 0.0	0.8 ± 0.0	0.4 ± 0.0	0.9 ± 0.0
Total phenols (g GAE/L)	0.4 ± 0.0	0.1 ± 0.0	0.1 ± 0.0	0.1 ± 0.0	0.4 ± 0.0	0.1 ± 0.0	0.3 ± 0.0

Notes: COD: Chemical oxygen demand, BOD: Biochemical oxygen demand, TOC: Total organic carbon, TS: Total solids, TVS: Total volatile solids, TDS: Total dissolved solids, TSS: Total dissolved solids, GAE: Gallic acid equivalent, TV: Tequila vinasse, FVW: Fruit-vegetable waste, CWW: Coffee wastewater, CCW: Crude cheese whey, TV-MPW: Tequila vinasse and maize processing wastewater, FVW-CCW: Fruit-vegetable waste and crude cheese whey, and TV-CCW: Tequila vinasse and crude cheese whey.

2.3. Experimental Setup and DF Conditions

Batch fermentations were carried out in a 5-L completely mixed reactor with a working volume of 3 L. As shown in Figure 1, the reactor was instrumented for the on-line monitoring and control of pH, mixing and temperature. The mixing rate was set at 100 rpm, while operational pH and temperature were kept constant at 5.5 ± 0.05 and 35 ± 1 °C, respectively. pH control was performed by automatically adding NaOH (10 M) or H₂SO₄ (1.8 M) solutions by means of a peristaltic pump. To start fermentation, the feedstock was initially fed to the reactor and supplemented (if any) according to the experimental condition (see Table 2). Then, the initial pH was adjusted to 5.5. After, the reactor was inoculated with 300 mL of activated inoculum (10% *v/v*); the pH was re-adjusted to 5.5 if needed. It is worth mentioning that no flushing was performed to deplete the initial residual oxygen, thus anaerobic conditions were achieved naturally by the action of facultative bacteria. Finally, a leak-proof test was subsequently conducted to ensure no gas loss during fermentation. During the operation, liquid samples were sampled throughout the fermentation with a 15-mL plastic hypodermic syringe and immediately stored in Eppendorf tubes at -20 °C until being analyzed for organic acids. Gas samples from the headspace were also collected periodically by using a 500-μL sample-lock syringe to determine the composition of the acidogenic off-gas (i.e., H₂, CH₄, and CO₂). The volume of off-gas that evolved was measured with a digital gas flow meter (Bioprocess control, Lund, Sweden). The cumulative hydrogen production was modelled with the modified Gompertz model (Equation (1)). Diauxic hydrogen production was, when observed, modelled by a two consecutive step approach according to Equation (2) [25] where H is the cumulative hydrogen production (NmL), λ is the lag-phase time (h), t is the culture time (h), P is the hydrogen production potential (NmL), R_m is the maximum hydrogen production rate (NmL/h), and e is Euler's number (≈2.7182). In Equation (2), the subscripts 1 and 2 denote the first and second hydrogen production steps. The volume of acidogenic off-gas was standardized at 0 °C and 1 atm, which are standard temperature and pressure conditions. All the fermentations were conducted in triplicate, giving the average and standard deviation values.

$$H = P \exp \left\{ -\exp \left[\frac{R_m e}{P} (\lambda - t) + 1 \right] \right\} \quad (1)$$

$$H = P_1 \exp \left\{ -\exp \left[\frac{R_{m1} e}{P_1} (\lambda_1 - t) + 1 \right] \right\} + P_2 \exp \left\{ -\exp \left[\frac{R_{m2} e}{P_2} (\lambda_2 - t) + 1 \right] \right\} \quad (2)$$

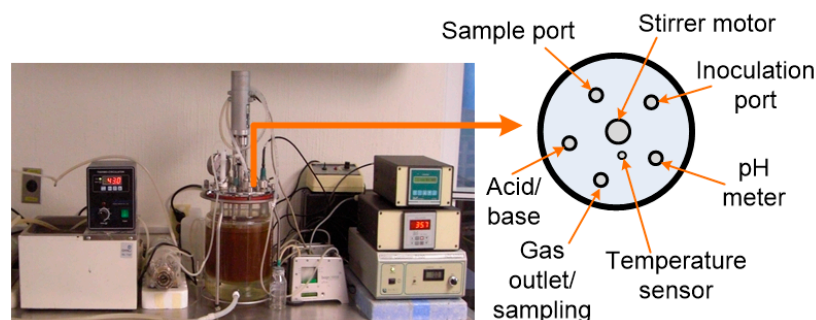


Figure 1. Photograph of the setup utilized for dark fermentations and schematic view of the reactor's cover. Adapted from [26]. Copyright 2019, with permission from Elsevier (License number: 5614750431682).

Table 2. Summary of nutrient supplementation applied in the feedstocks.

Feedstock	Nutrient Supplementation (g/L)	Fed Volume (L)
FVW	NH ₄ Cl, 2.4; K ₂ HPO ₄ , 2.4; MgSO ₄ ·7H ₂ O, 1.5; KH ₂ PO ₄ , 0.6; CaCl ₂ , 0.11; FeSO ₄ ·7H ₂ O, 0.05	1.2 ^a
CCW	Without nutrient supplementation	2.7
CWW	NH ₄ Cl, 2.4 and FeSO ₄ ·7H ₂ O, 0.05	2.7
TV	NH ₄ Cl, 2.4 and FeSO ₄ ·7H ₂ O, 0.05	2.7
TV-MPW	Without nutrient supplementation	2.7
TV-CCW	FeSO ₄ ·7H ₂ O, 0.05	2.7
CCW-FVW	Without nutrient supplementation	2.7

Note: ^a 1.5 L of distilled water was supplied to achieve a suitable fermentation broth to be mixed properly.

2.4. Oxygen Depletion Test

The ability of the biocatalyst to help the process in achieving a suitable reducing environment was indirectly tested by tracking the concentration of dissolved oxygen (DO) in the broth over time. Two oxygen depletion tests were performed, one during the pre-fermentation step (which is the step aimed at activating dormant bacteria) and the other one during the inoculation step. Both tests were carried out in the same 3-L instrumented reactor equipped with a DO sensor (Part No. z010023525; Applikon Biosciences, Schiedam, The Netherlands). The DO concentration was measured and recorded using the BioXpert Lite software (version 1.13). The calibration of the sensor was performed according to the manufacturer's guide. The pre-fermentation step was conducted using the mineral growth medium previously described in Section 2.1 but under oxygen saturation conditions. The pre-fermentation step used TV as feedstock for demonstration purposes. For both steps, the temperature, pH, and mixing rate conditions were maintained constant as those previously specified in Section 2.3. An abiotic control (without inoculum) was also performed.

2.5. Self-Fermentation Test

For comparison purposes and in order to validate the inoculum's bioactivity (functionality of the biocatalyst), two self-fermentation experiments consisting of the dark mono-digestion of CCW and FVW were carried out under the same conditions and using the setup described previously in Section 2.3 but without the addition of inoculum. Both CCW and food waste have been reported to support self-fermentation [25,27]. The microbial community that evolved during self-fermentation was explored and qualitatively compared with that of the biocatalyst. Microbial sampling was performed during the maximum hydrogen production rate.

2.6. Analytical Methods

The chemical oxygen demand (COD), biochemical oxygen demand (BOD), pH, alkalinity, acidity, total nitrogen, total phosphorus, sulfate, and solids were analyzed according

to standard methods [28]. Total organic carbon, total carbohydrates, total reducing sugars (TRS), phenolic compounds, and the acidogenic off-gas composition were measured as previously reported by [17]. The soluble metabolite products, namely, acetate, propionate, butyrate, iso-butyrate, and lactate, were measured by high-performance liquid chromatography (HPLC) using a Varian ProStar™ HPLC system model 230 (Varian Analytical Instruments, Palo Alto, CA, USA), which was equipped with Varian 325 UV-VIS detector and a column Aminex HPX-87H (300 mm × 7.8 mm id, 9 μm; Bio-Rad, Hercules, CA, USA). The column temperature was maintained at 55 °C. The mobile phase was a solution of sulfuric acid (5 mM) at a flow rate of 0.5 mL/min. The organic acids were measured using a wavelength of 210 nm.

The microbial community structure of the biocatalyst and of the self-fermentation of CCW and FVW was analyzed by short-length 16S rRNA gene sequencing (Illumina, San Diego, CA, USA). Genomic DNA was isolated using the MoBio PowerSoil® DNA Extraction Kit (Mo Bio Laboratories Inc., Carlsbad, CA, USA) according to the manufacturer's instructions. The amount and quality of the extracted DNA were determined using the NanoDrop-2000 Spectrophotometer (Thermo Fisher Scientific, Wilmington, DE, USA). The isolated DNA was stored at −80 °C until DNA samples were sent to the Research and Testing Laboratory (RTL, Austin, TX, USA) for sequencing. The primer set 28F (GAGTTTGATCNTGGCTCAG) and 388R (TGCTGCCTCCCGTAGGAGT) and the Illumina MiSeq platform were utilized. Bioinformatic analysis was conducted according to the RTL protocol previously described elsewhere [29].

3. Results and Discussion

3.1. Hydrogen Production Performance

In the inoculum-aided DF, the highest and lowest cumulative hydrogen production values were observed with CCW (19.1 NL H₂, corresponding to 7.1 NL H₂/L_{feedstock} or 1.65 mol H₂/mol hexose) and CWW (0.5 NL H₂, corresponding to 0.2 NL H₂/L_{feedstock} or 0.51 mol H₂/mol hexose), respectively (Figure 2a). The second highest hydrogen production was recorded when fermenting FVW, averaging 9.1 NL H₂, which was equivalent to 7.5 NL H₂/L_{feedstock} or 1.72 mol H₂/mol hexose. TV yielded 1.3 NL H₂/L_{feedstock} (0.82 mol H₂/mol hexose). Compared to the literature, the hydrogen yield from CCW, on a fresh feedstock basis, was found to be higher than the 5.3 NL H₂/L_{feedstock} reported by Asunis et al. (2022) from sheep CCW or the 3.7 NL H₂/L_{feedstock} recently reported by Aranda-Jaramillo et al. (2023) from delipidated acid CCW from cow's milk [30,31]. The hydrogen production from TV was 3.7 times lower than that obtained previously in batch mode by García-Depraect and León-Becerril (2018) [24], likely due to the differences existing in the operational pH (here fixed pH of 5.5 versus a two-stage pH control starting at 6.5 and switched to 5.8 at the beginning of the accelerated hydrogen production phase). Regarding FVW, Martínez-Mendoza et al. (2023) achieved up to 9.4 NL H₂/L_{feedstock} in a continuously stirred tank reactor (CSTR) operated at 9 h hydraulic retention time (HRT) and 37 °C; such a hydrogen conversion yield is 25% higher than that obtained in batch mode in the present study [32]. In another study, Martínez-Mendoza et al. (2022) achieved hydrogen yields between 3.7 and 6.6 NL H₂/L_{feedstock} using a mixture of FVW in lactate-driven DF tests conducted under batchwise mesophilic conditions at different operational pH (5.5, 6.0, 6.5, and 7.0), initial total solids (5 and 7%), and initial cell biomass concentrations (18, 180, and 1800 mg volatile suspended solids/L) [12]. Finally, the hydrogen production yield achieved from CWW was comparatively similar to that previously reported for this type of feedstock [33]. Montoya et al. (2019) investigated the hydrogen production via DF from CWW in combination with coffee pulp and husk, recording a maximum hydrogen potential of 328 NmL H₂/L of feedstock (2 g/L pulp and husk + 30 g COD/L CWW + 2 g/L yeast extract) at 30 °C and initial pH 7.0 (5.9 final pH) [33]. One of the reasons for the relatively low hydrogen yield herein obtained from CWW is the low concentration of carbohydrates, which are the primary source of hydrogen. Indeed, the carbohydrate content of CWW was

determined to be approximately 20, 15, and 8.5 times lower than that of FVW, CCW, and TV, respectively (Table 1).

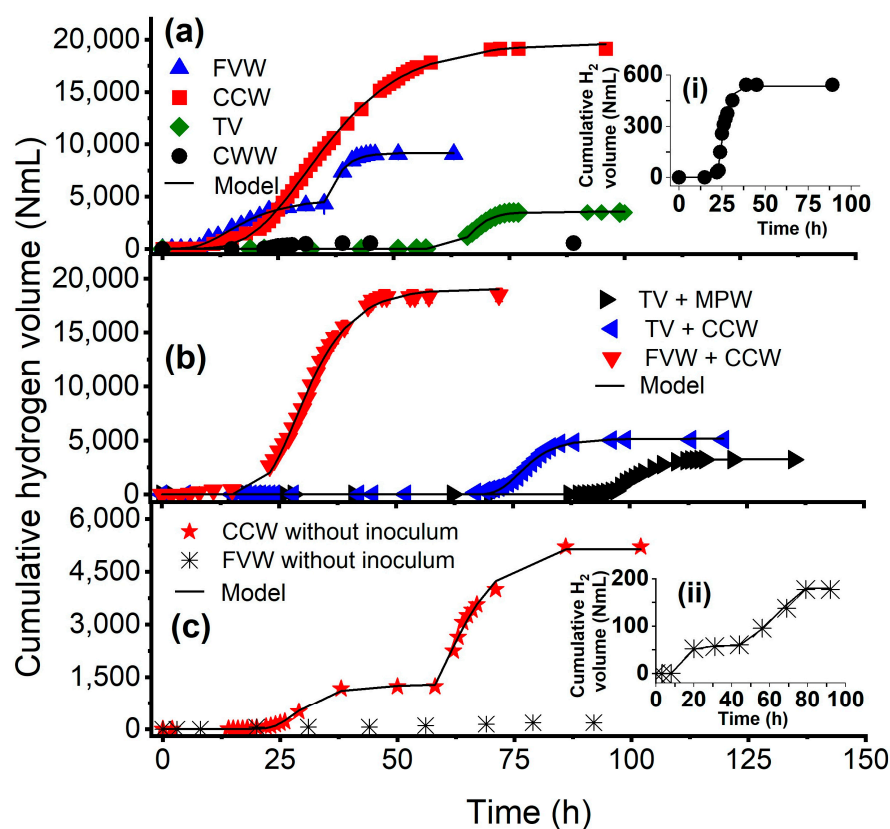


Figure 2. Cumulative hydrogen production with and without addition of inoculum. (a) Mono-fermentation with inoculation of food-vegetable waste (FVW), crude cheese whey (CCW), tequila vinasse (TV), and coffee wastewater (CWW); (b) co-fermentation with inoculation of TV + MPW, TV + CCW, and FVW + CCW; (c) mono-fermentation without inoculation of CCW and FVW. Inserted graphs represent the close-up of (i) CWW and (ii) FVW.

Regarding the dark co-fermentation tests (Figure 2b), the mixture of 80% TV and 20% MPW resulted in a comparable hydrogen production yield ($1.2 \text{ NL H}_2/\text{L}_{\text{feedstock}}$ or $0.83 \text{ mol H}_2/\text{mol hexose}$) to the dark mono-fermentation of TV but without needing nutrient supplementation. Such a co-feedstock ratio (80/20 *w/w*) has been claimed as the optimal one, which resulted in a better balance of nitrogen, iron, magnesium, and phosphorus, as well as improved alkalinity due to the calcium carbonate-rich MPW [17]. However, in the present study, a synergy in nutrients was not highly evident from the physicochemical characterization performed. On the other hand, the co-fermentation of TV and CCW resulted in $1.9 \text{ NL H}_2/\text{L}_{\text{feedstock}}$ ($0.34 \text{ mol H}_2/\text{mol hexose}$); however, such a hydrogen yield was 30% lower than the theoretical one estimated from the corresponding dark mono-fermentation test. One explanation for that observation could be that TV and CCW were not compatible with each other. Finally, the co-fermentation of CCW and FVW enabled the production of $6.8 \text{ NL H}_2/\text{L}_{\text{feedstock}}$ or $1.75 \text{ mol H}_2/\text{mol hexose}$, which was 7% higher than the theoretical value, indicating some synergistic effect. Gómez-Romero and co-workers investigated the dark co-fermentation of CCW and FVW at five different C/N ratios (7, 17, 21, 31, and 46) in a 2-L completely mixed batch reactor at 5.5 pH and 37 °C [18]. The authors found the highest hydrogen production of $5.7 \text{ NL H}_2/\text{L}_{\text{feedstock}}$ at a C/N ratio of 21, as that ratio provided a better buffering capacity and an improved nutrient balance.

In general, the biocatalyst used in the DF enabled high hydrogen production outcomes depending on the feedstock used. In addition, it is highly probable that the hydrogen production activity is further improved when applying optimum operational conditions

in a continuous feeding mode. As shown in Table 3, the hydrogen production kinetic behavior in all the conditions tested was well described by the modified Gompertz model. Here it is worth mentioning that the DF of FVW showed a diauxic hydrogen production pattern, likely due to a temporal availability in different fermentable organics with specific metabolization rates. Such a two-step hydrogen production pattern has also been found in dark fermenters running on CCW at pH values ranging from 5.5 to 7.5 [25]. In inoculum-aided fermentations, the length of lag phase varied from 7.7 to 95.5 h depending on the feedstock type. FVW showed the shortest adaptation period due to its high content in rapidly available fermentable carbohydrates. Regarding the maximum volumetric hydrogen production rate ($VHPR_{max}$), the highest value (393 NmL H₂/L-h) was observed with FVW, particularly at the second step of the diauxic hydrogen curve. The second fastest $VHPR_{max}$ (343 NmL H₂/L-h) was observed in the dark co-fermentation of FVW-CCW. Approximately 200 NmL H₂/L-h was recorded with CCW, while TV sustained a $VHPR_{max}$ of 152 NmL H₂/L-h. The lowest $VHPR_{max}$ of 24 NmL H₂/L-h was achieved with the use of CWW, as discussed above, most likely due to its low fermentable organics content.

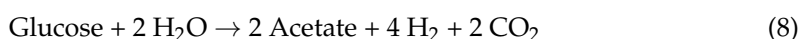
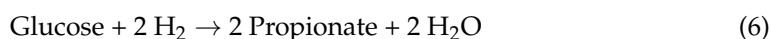
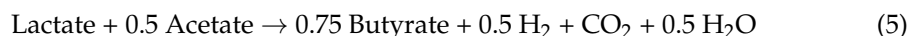
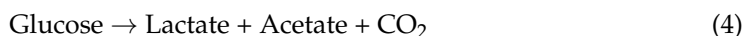
Table 3. Hydrogen production kinetic behavior of the different feedstocks and dark fermentation (DF) conditions assessed.

DF Type	Feedstock	P, NmL	$VHPR_{max}^c$, NmL H ₂ /L-h	λ , h	R ²
Inoculum-aided mono-fermentation	FVW	4556.0 ^a , 9157.7 ^b	84.8 ^a , 393.3 ^b	7.7 ^a , 31.4 ^b	0.9885
	CCW	19,673.0	199.8	18.8	0.9991
	TV	3537.3	151.8	63.5	0.9984
	CWW	534.2	24.2	22.0	0.9899
Inoculum-aided co-fermentation	TV-MPW	3281.7	94.7	95.5	0.9991
	TV-CCW	5163.9	138.5	71.6	0.9947
	FVW-CCW	19,066.1	342.6	21.7	0.9975
Self-fermentation	CCW	1257.0 ^a , 5263.5 ^b	32.9 ^a , 92.7 ^b	23.6 ^a , 53.46 ^b	0.9982
	FVW	59.3 ^a , 188.7 ^b	2.2 ^a , 1.8 ^b	9.9 ^a , 37.9 ^b	0.9964

Note: Some conditions tested, namely the type of DF and feedstock led to a diauxic hydrogen production pattern over time; superscripts ^a and ^b denote the kinetic parameter estimated during the first and second hydrogen production steps. ^c $VHPR_{max}$ (maximum volumetric hydrogen production rate) is R_m (maximum hydrogen production rate) divided by working volume.

As for the profile of organic acids during DF, a two-step lactate-type fermentation was observed in all the inoculum-aided fermentation tests regardless of the DF type (i.e., mono- or co-fermentation), except when feeding CWW (Figure 3a–g). The dual-phase lactate fermentation was characterized by the first fermentation of carbohydrates (Equations (3) and (4)) mainly into lactate (which explains the stepped-up amounts of lactate observed during the early fermentation stage), followed by the second fermentation of lactate (Equation (5)) which produces hydrogen, butyrate, and carbon dioxide (which explains the sudden decrease observed in the broth lactate concentration, which indeed matched well with the hydrogen and butyrate co-production). Dual-phase lactate fermentation has been well documented with the use of TV [14,17], simulated CW [34], food waste [13], FVW [12], and CCW [35], among others. It is noteworthy that lactate can be produced and oxidized simultaneously by fashioned syntrophic interactions between LAB and LO-HPB [10,31], as will be discussed in Section 3.4. As descriptive data, peaked lactate titers were in the range of 13.1 to 36.4 g/L. The co-fermentation of FVW and CCW showed the highest lactate titer, which averaged 36.4 g/L. It was assumed that the high titer was mainly derived from CCW rather than from FVW, as the former co-feedstock resulted in up to 33.3 g lactate/L while the latter one only enabled a peak lactate concentration slightly above 12 g/L. The use of TV, FVW, TV-MPW, and TV-CCW led to similar lactate titers (c.a. 13–15 g/L). In contrast, CWW only showed an average initial lactate concentration of 5.5 g/L, but afterward, it

declined over the fermentation period down to 0.1 g/L. Regarding butyrate, its maximum titer ranged from 3.3 to 13.9 g/L, the lowest and highest value was recorded with CWW and CCW-FVW, respectively, yet CCW alone showed a quite similar concentration that its co-fermentation counterpart with FVW. It is not surprising that a positive correlation between hydrogen production and butyrate accumulation was observed, as butyrate is the main soluble by-product produced from the most common lactate-driven DF pathway (Equation (5)) [10]. It is also important to note that besides lactate and butyrate, other organic acids were detected throughout fermentation, such as acetate and propionate (Figure 3). The concentration of acetate remained at lower levels, below approximately 3 g/L. Notably, in some runs (i.e., TV, TV-PMW, and TV-CCW), acetate suddenly decreased in parallel with the depletion of lactate. It is known that acetate acts as an acceptor electron during the oxidation of lactate [10], thus explaining the low levels of acetate and its pronounced decrease during the second lactate-type fermentation. At the late fermentation stage, we also observed a slight accumulation of propionate, which agreed with previous works [12,13,26,36]. Propionate formation is not desirable because it is a hydrogen sink; indeed, it is metabolically possible to produce propionate from fermentable carbohydrates (Equation (6)) and from lactate (Equation (7)), both compounds can be hydrogen precursors (Equations (5), (8) and (9)) [29,37]. Although different complex feedstocks were assessed, the consistency observed in the metabolic pathways involved in the dual-lactate DF fermentation is a finding of great significance for the ongoing development of DF.



3.2. Oxygen Depletion during Activation and Inoculation Steps

The oxygen depletion capacity of the biocatalyst utilized was investigated during the pre-fermentation and inoculation steps. In the pre-fermentation step, we observed a complete oxygen consumption within the first 2–3 h of incubation despite the fact that the mineral growth medium was previously saturated with oxygen to 6.84 mg O₂/L (Figure 4). The DO in the abiotic control remained stable (between 95.5 and 100%) throughout the experiment, pointing out the good capacity of the inoculum to achieve anoxic conditions. During the pre-fermentation stage, the initial pH of 6.2 remained constant within the first 3.5 h culture, but it markedly dropped down to 4.1 after 10 h, then it slowly decreased afterward to a final value of 3.7 (Figure 4). It is noteworthy that the biocatalyst used exhibited a high tolerance against acid pH, indicating that it can withstand unforeseen acidification disturbances, which might occur in DF systems [38,39]. As shown in Figure 4, the oxygen concentration suddenly increased to 2.74 mg O₂/L (40 ± 2.4%) during inoculation, but it was rapidly depleted within the 5 min culture. Interestingly, high variability in the oxygen consumption rate was recorded during the pre-fermentation step as compared to that obtained during the inoculation one, likely due to more active facultative anaerobes.

It can be hypothesized that bacteria present in the inoculation step were metabolically more active than dormant bacteria, thereby depleting immediately the residual oxygen. To sum up, the results obtained confirmed that the biocatalyst used was able to create an anoxic environment, which is of great significance to allow the growth of obligate anaerobes producing hydrogen such as *Clostridium* spp. [40].

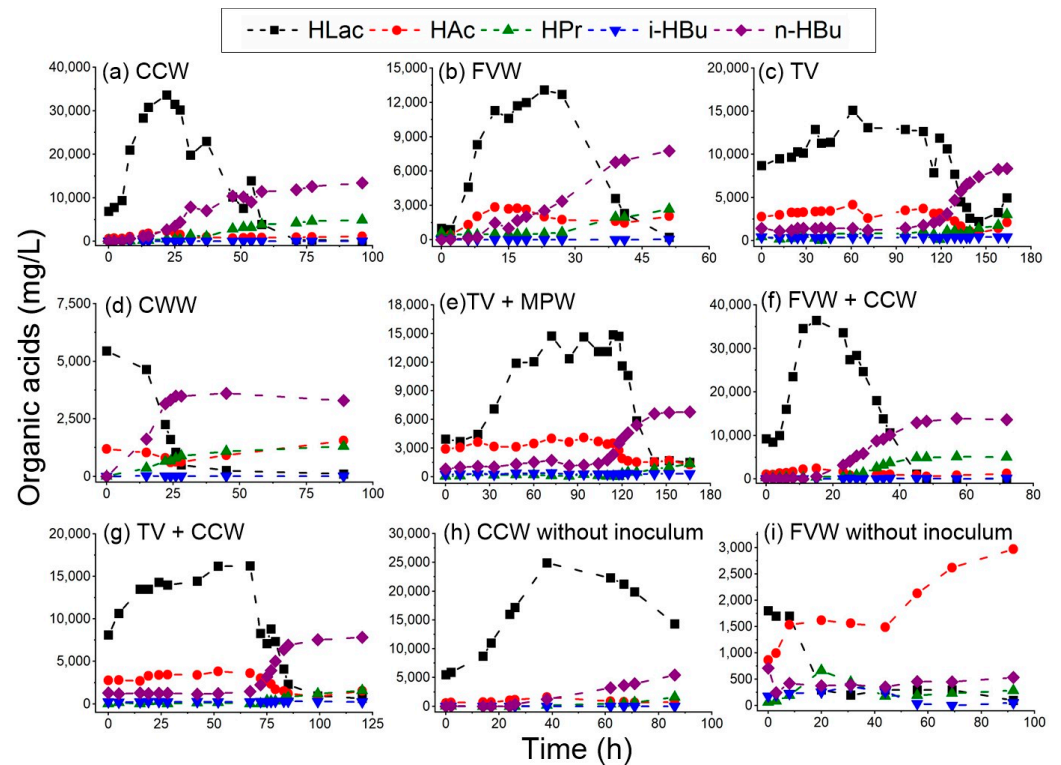


Figure 3. Profile of organic acids accumulated during dark (a–g) fermentation and (h,i) self-fermentation. HLac: Lactate, HAc: Acetate, HPr: Propionate, i-HBu: Iso-butyrate, n-HBu: Butyrate.

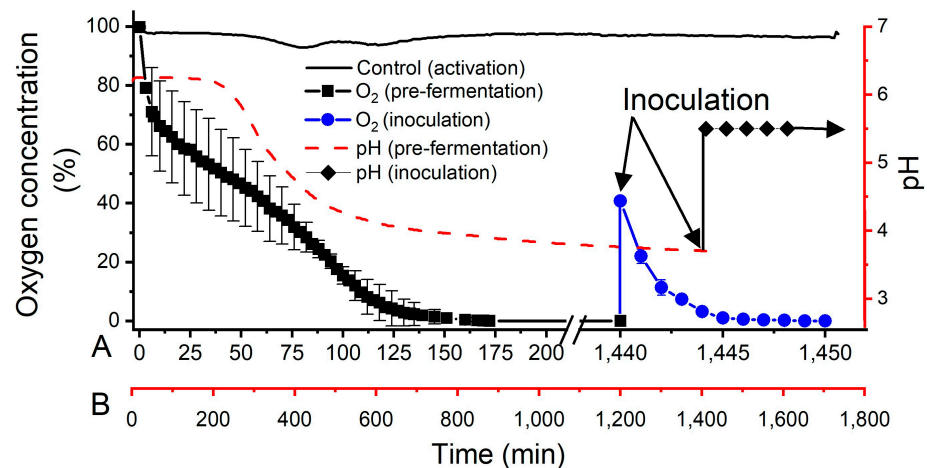


Figure 4. Time evolution of pH and dissolved oxygen during the activation and inoculation steps (100% [O₂] corresponds to saturated conditions, 6.84 mg/L). Dissolved oxygen is graphed in the primary x-axis (A), while pH is graphed in the secondary one (B).

The ability to deplete residual oxygen either during the start-up or just after unintentional oxygen supply is highly desirable, as hydrogen production via DF is quite sensitive to oxygen [8,40]. Facultative anaerobes are oxygen-consuming species; however, their presence in dark fermenters is often limited because of the application of severe

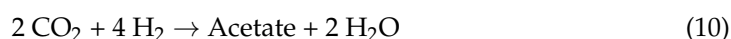
pretreatments (e.g., heat shock) to the substrate and/or inoculum [8,41,42]. Perhaps this reasoning may explain why anoxic conditions achieved naturally (by the action of the microflora) have seldom been reported [17,43,44]. In this study, we detected the presence of facultative bacteria such as *Klebsiella* sp., *Enterobacter* sp., and *Lactobacillus* spp., among others, as will be presented and discussed in more detail in Section 3.4. The pretreatment applied herein resulted in a highly specialized inoculum composed of both facultative and strictly anaerobic bacteria [14,23,24]. From a practical point of view, the exploitation of this biocatalyst (and others with similar functionality) can decrease operating costs by avoiding the implementation of any artificial method devoted to achieving anoxic conditions, such as the flushing of inert gasses or the addition of chemical-reducing agents.

3.3. Testing the Dark Self-Fermentation of Crude Cheese Whey and Fruit–Vegetable Waste

The DF driven by the indigenous microorganisms present in the substrate is known as self-fermentation. This study assessed the dark self-fermentation of CCW and FVW and compared both the hydrogen production performance and the profile of organic acids (metabolic pathways) involved with those observed in the inoculum-assisted DF. As shown in Figure 2c, the hydrogen production potential was 5202.5 NmL (1926.9 NmL H₂/L_{feedstock} or 0.45 mol H₂/mol hexose) and 177.9 NmL (148.3 NmL H₂/L_{feedstock} or 0.03 mol H₂/mol hexose) for CCW and FVW, respectively. Such amounts represented only 27.2 and 2.0% of the total amount of hydrogen produced in the inoculum-aided DF of CCW and FVW, respectively. Like the DF runs performed with inoculation, methane was not detected during the whole self-fermentation period, likely because of the high initial substrate-to-microorganism ratio, which favors the development of HPB with a rapid growth rate over methanogens with slower growth rates [20,44]. The findings herein observed reinforce the idea that FVW and CCW not only serve as substrates but also as sources of HPB [44,45]. As for hydrogen modelling, the experimental data were well represented by the model used, obtaining good correlation values (Table 3). Significant differences in the hydrogen production kinetics attained with and without inoculation were also found (Table 3). For instance, compared to fermentations with inoculation, the VHPR_{max} of FVW and CCW decreased from 393.3 to 2.2 NmL H₂/L-h and from 199.83 to 92.7 NmL H₂/L-h, respectively. The lag phase was estimated as 9.9 h for FVW and 23.6 h for CCW, both slightly longer than its inoculum-aided DF counterpart. Interestingly, diauxic hydrogen production was also observed for the self-fermentation of FVW. In contrast, for CCW, a diauxic hydrogen production profile was only observed in the DF without inoculation, which could be attributed to reduced hydrolytic activity of indigenous microflora. In contrast, the inoculum-aided DF of FVW showed, by visual inspection, a marked change in the rheology/appearance of the broth. In the beginning, the broth presented particulate organics, which were later not appreciated. Apparently, the broth was less viscous as incubation time proceeded, pointing out the high hydrolytic activity of the inoculum used.

Figure 3h,i depicts the organic acids measured during the self-fermentation of CCW and FVW. In general, the hydrogen production from CCW followed the lactate-driven DF metabolic pathway (via dual-phase lactate fermentation). Interestingly, in the case of FVW, at the end of fermentation, the major organic acid was acetate (2972.5 mg/L) with small amounts of lactate (100 mg/L), propionate (288.9 mg/L), iso-butyrate (52.9 mg/L), and butyrate (537.5 mg/L), pointing out strong differences in the diversion of electron flux when compared to DF with inoculation. Particularly, the initial lactate concentration of 1800 mg/L remained stable during the first 8 h culture, but then it was decreased to approximately 300 mg/L after 20 h culture and remained nearly constant thereafter. It was therefore suggested that lactate consumption was implicated in the first hydrogen production stage. On the other hand, the initial acetate concentration of 864.7 mg/L rose on average to 1624.4 mg/L after 20 h of fermentation and remained virtually constant after 44 h culture, but then it increased again up to approximately 2970 mg/L. The high acetate/butyrate ratio (3.25 on a COD basis), as well as the diauxic generation of acetate, indicated that acetic

acid-type fermentation (Equation (8)) was involved in the second hydrogen production stage. The high levels of acetate along with the low amounts of hydrogen that evolved also suggested the presence of homoacetogenesis, an undesirable metabolic pathway in DF that implies the consumption of 4 mol hydrogen and 2 mol of carbon dioxide to form 1 mol of acetate (Equation (10)) [46]. In contrast, as previously discussed, acetate had a different behavior in the inoculated DF runs, since it mostly tended to decrease along with lactate. Altogether, the autochthonous microflora and the inoculum used showed quite different process performances from each other. The biocatalyst employed enabled us to tailor the metabolic flux during the fermentation of several agro-industrial resources, not only leading to lactate but also to hydrogen and butyrate through a fashion dual-phase lactate fermentation.



3.4. Microbial Community Structure

Gaining an in-depth understanding of the microbial community structure of hydrogen-producing inocula is a keystone in biocatalyst management, as well as improving DF efficiency since the microbial composition greatly impacts the process. The present work explored the inoculum's microbial structure but also the microbiology that evolved during self-fermentation. As shown in Figure 5, the inoculum showed a high level of organizational structure since more than 90% of microbial abundance was represented by 20% of the species detected. This microbial distribution was consistent with the Pareto principle stating that roughly 20% of the species are covered by 80% of the total community abundance [47]. Based on the metabolic capacity, the bacteria were divided into three groups, namely, HPB, LAB and acetic acid bacteria (AAB). The relative abundance was 85.9, 5.7 and 5.8% for HPB, LAB, and AAB, respectively [14]. Note that the group of LAB was left out from the HPB one; however, some LAB have been reported to be able to produce hydrogen [48–50]. Also, it should be noted that the microbial analysis was performed at a species level for the first analysis, but the final species taxonomy should be determined by means other than molecular analysis like long-read sequencing. The microbial structure of the initial inoculum generally changes throughout the fermentation time, being impacted by the type of substrate and operational conditions. In this work, the “guild” is mainly composed of HPB, LAB, and AAB (Figure 5). These microbial groups have been previously identified as the principal core group enabling the production of hydrogen from lactate and acetate via cross-feeding interactions (Figure 6) [17,31]. *Clostridium* and LAB have been reported to be dominant in DF and important to driving the hydrogen production process forward, even after a long time [23].

Among HPB, *Clostridium beijerinckii* (36.0%), *Actinomyces* sp. (21.6%), and *Enterobacter* sp. (17.8%) comprised more than 75% of the total reads. Moreover, *Clostridium* sp., *Klebsiella pneumoniae*, *C. butyricum*, and *Citrobacter* sp. represented 6.1, 3.1, 3.0, and 2.2%, respectively. As for LAB, *Lactobacillus casei* and *L. harbinensis* were the most abundant species, accounting for 58.8 and 31% of the total reads belonging to LAB, respectively. Other less abundant species such as *Streptococcus* sp. (8.7%) and *L. parabuchneri* (0.8%) were also found. Regarding AAB, a less-diverse microbial group represented by the genus *Acetobacter* was observed, including *Acetobacter lovaniensis* (81.2%) and other unknown species (18.8%). Low hydrogen production can be produced by the presence of homoacetogens according to Equation (10). However, here no acetate accumulation was observed. Conversely, acetate consumption was correlated to hydrogen production. The little or lack of presence of carbon dioxide during the first lactate-type fermentation suggested that AAB could be considered helpers since they can generate the acetate necessary to support the reaction described in Equation (5), where 0.4–0.53 mol of acetate is necessary for each mol of lactate oxidized to form 0.47–0.62 mol of hydrogen and 0.66–0.83 mol of butyrate [10]. This observation corresponds with that of Tao et al. (2016), who reported the addition of exogenous acetate favored lactate consumption and butyrate formation when using a LO-HPB, i.e., *Clostridium* sp. BPY5 [19].

Therefore, the stimulant effect of AAB involved in the production of hydrogen from lactate seemed to exceed the antagonistic impact associated with the homoacetogenic pathway.

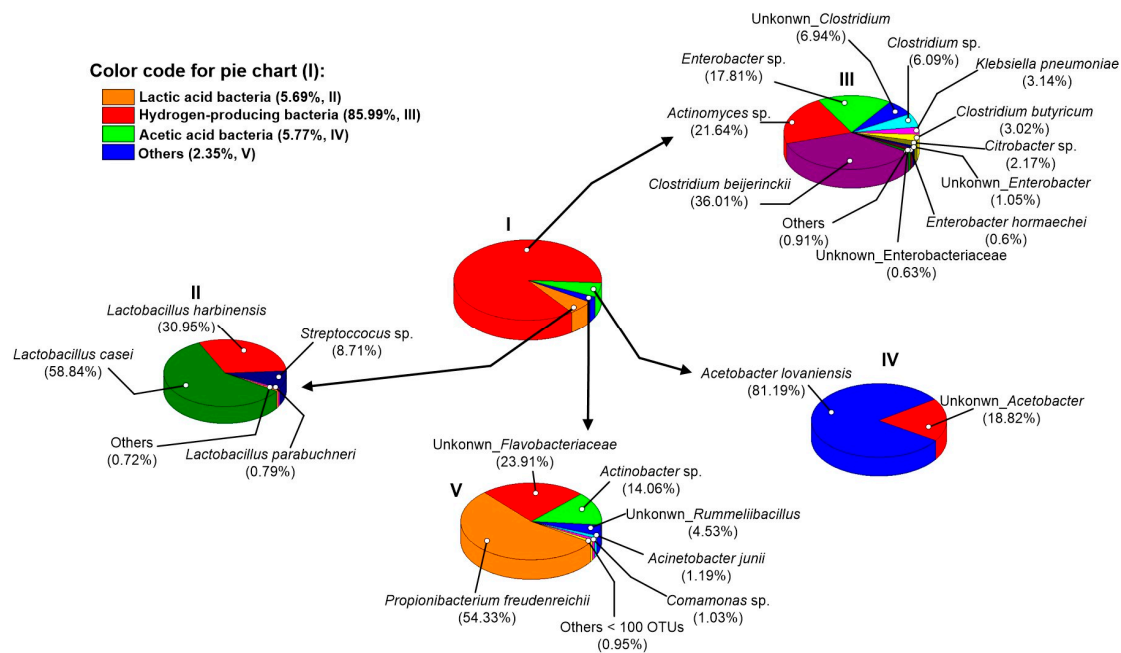


Figure 5. Microbial community structure at genus level of the biocatalyst used. For interpretation of the references to color in this figure legend, the reader is referred to the Web version of this article.

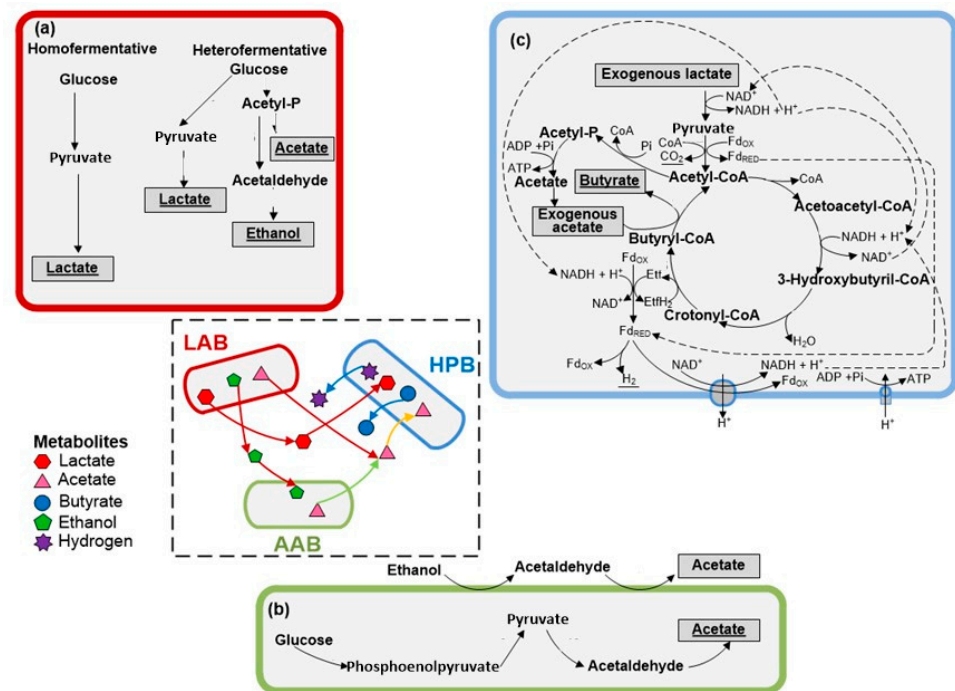


Figure 6. Schematic representation of (a) homo- and hetero-lactic fermentation by lactic acid bacteria (LAB), (b) the oxidation of glucose and ethanol by acetic acid bacteria (AAB), and (c) the production of hydrogen from the oxidation of lactate by hydrogen-producing bacteria (HPB). Putative lactate- and acetate-based cross-feeding interactions between LAB, AAB, and HPB are denoted inside the dotted rectangle. Figure reused with the kind permission of authors referred to in reference [31].

Regarding the microbial community of self-fermentations, approximately two-thirds of the total reads were covered by LAB when using CCW (Figure 7). Bacteria belonging

to HPB had a share of 20.4%. In the case of FVW, 77.2% of total reads were closely affiliated with HPB, while *L. harbinensis* (1.4%) was the only representative of the LAB group. Interestingly, the AAB group was not identified either with CCW or with FVW. *L. casei* (the dominant bacteria identified in the biocatalyst) was not found in both self-fermentations tested. Instead, CCW had *L. helveticus* (50.1%), *L. delbrueckii* (16.0%), *L. lactis* (7.7%), and *L. fermentum* (1.7%). Another interesting finding observed is that, like the biocatalyst used, CCW also harbored *C. butyricum* (1.1%) and *C. beijerinckii* (4.8%), two well-known LO-HPB. Such LO-HPB endorsed the lactate-driven DF observed in the self-fermentation of CCW. Thus, CCW can be considered a good source not only of LAB but also of LO-HPB. *Enterobacter* and *Actinomyces* genera were also absent in the dark self-fermentation of CCW, highlighting the differences existing between the biocatalyst used and the endogenous microflora that evolved. *Blautia* genus, recognized as homoacetogen [29], was detected in FVW, which can explain the high acetate concentrations recorded in the dark self-fermentation of FVW along with the poor hydrogen production outcome. From our findings, it can be concluded that the microbial community structure of the inoculant used was of utmost importance to steer the fermentation towards a dual-phase lactate fermentation, even using different complex agro-industrial resources, each containing several different endogenous bacteria.

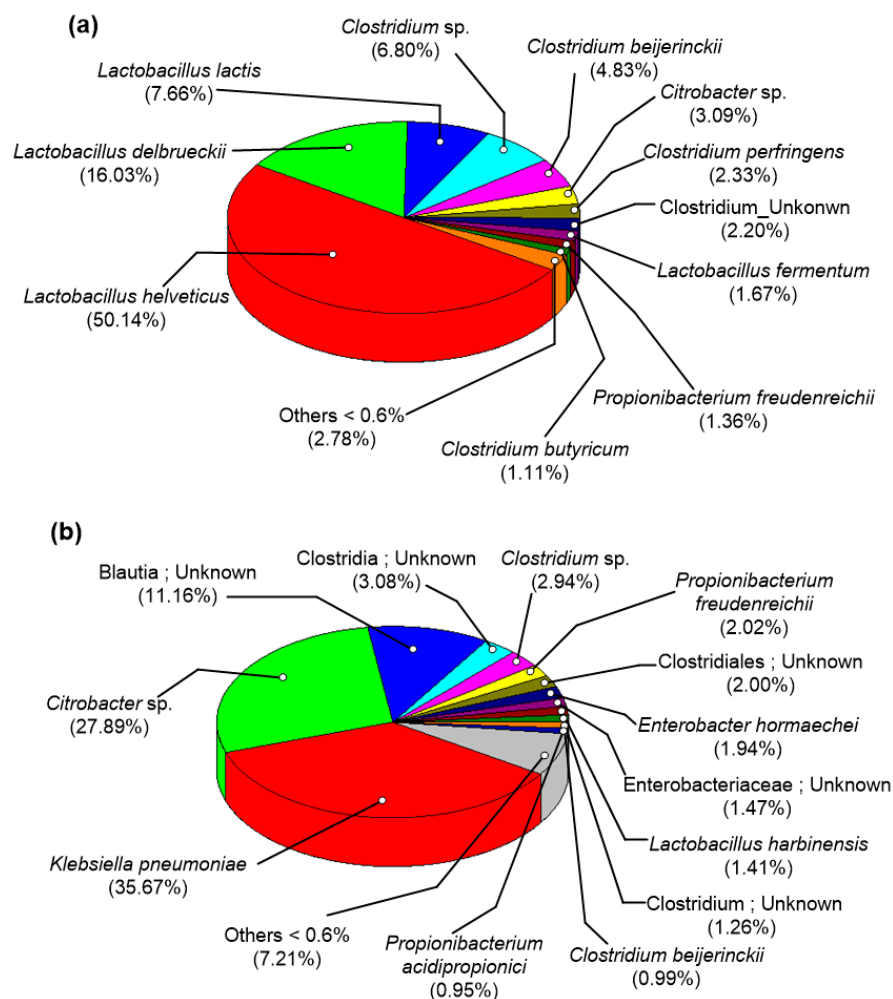


Figure 7. Indigenous microflora of the dark self-fermentation of (a) crude cheese whey and (b) fruit-vegetable waste. Both samples were drawn during the highest hydrogen production rate and analyzed by short-read 16S rRNA sequencing.

4. Conclusions

The use of a highly specialized biocatalyst was successfully tested to steer the dark mono- and co-fermentation of different agro-industrial resources towards dual-phase lactate fermentation. The target products derived from the tailored two-step lactate fermentation were lactate and hydrogen and butyrate. Hydrogen and butyrate were co-produced efficiently but had a trade-off against lactate. The biocatalyst used was not only able to achieve anoxic conditions by removing residual oxygen but also to hydrolyze particulate organics. Among the different feedstocks tested, CCW and FVW, alone or in co-fermentation, stand out as the most suitable ones to be subjected to DF. A totally different process performance, in terms of the metabolic pathway and the target product peak titer, was observed when comparing inoculum-aided fermentations and self-fermentations. Significant higher product titers were attained in inoculated DF tests, leading to lactate and butyrate peak concentrations between 13.1 and 36.4 g/L and between 3.3 and 13.9 g/L, respectively. Hydrogen yields were in the range of 0.2 to 7.5 NL H₂/L_{feedstock} (0.3–1.7 mol H₂/mol hexose), depending on the feedstock type. From process characterization and microbial analysis, it can be concluded that the microbial community structure was key in dictating the fermentation performance. Although the microbial community structure of the self-fermentation and biocatalyst used herein shared some bacteria, the biocatalyst had its own microbial organizational structure. Bacteria belonging to the LAB, LO-HPB, and AAB groups were keystones in the biocatalyst. The significance of this work lies in the fact that the biocatalyst assessed can be employed as a workhorse for the valorization of agro-industrial resources via DF. The findings of the present study and their discussion constitute a step further in DF inoculum management.

Author Contributions: Conceptualization, validation, formal analysis, data curation, methodology, O.G.-D. and E.L.-B.; investigation, writing—original draft preparation, O.G.-D.; writing—review and editing, funding, E.L.-B. All authors have read and agreed to the published version of the manuscript.

Funding: This work was supported by CONAHCYT (CONACYT-Project-PN-2015-01-1024). Octavio García-Depraect is supported by Grant RYC2021-034559-I funded by MCIN/AEI/10.13039/501100011033 and by European Union NextGenerationEU/PRTR. The regional government of Castilla y León and the European FEDER Programme (CL-EI-2021-07 and UIC 315) are also acknowledged.

Data Availability Statement: Data will be made available upon request.

Acknowledgments: This work is dedicated to the everlasting memory of the late Alberto López López and Jacob Gomez Romero.

Conflicts of Interest: The authors declare no conflict of interest.

References

1. Patel, S.K.; Das, D.; Kim, S.C.; Cho, B.-K.; Kalia, V.C.; Lee, J.-K. Integrating strategies for sustainable conversion of waste biomass into dark-fermentative hydrogen and value-added products. *Renew. Sustain. Energy Rev.* **2021**, *150*, 111491. [[CrossRef](#)]
2. Sekoai, P.T.; Ghimire, A.; Ezeokoli, O.T.; Rao, S.; Ngan, W.Y.; Habimana, O.; Yao, Y.; Yang, P.; Fung, A.H.Y.; Yoro, K.O.; et al. Valorization of volatile fatty acids from the dark fermentation waste Streams-A promising pathway for a biorefinery concept. *Renew. Sustain. Energy Rev.* **2021**, *143*, 110971. [[CrossRef](#)]
3. Garcia-Navarro, J.; Isaacs, M.A.; Favaro, M.; Ren, D.; Ong, W.J.; Grätzel, M.; Jiménez-Calvo, P. Updates on hydrogen value chain: A strategic roadmap. *Glob. Chall.* **2023**, 2300073. [[CrossRef](#)]
4. Balachandar, G.; Varanasi, J.L.; Singh, V.; Singh, H.; Das, D. Biological hydrogen production via dark fermentation: A holistic approach from lab-scale to pilot-scale. *Int. J. Hydrogen Energy* **2020**, *45*, 5202–5215. [[CrossRef](#)]
5. Patel, S.K.; Gupta, R.K.; Das, D.; Lee, J.K.; Kalia, V.C. Continuous biohydrogen production from poplar biomass hydrolysate by a defined bacterial mixture immobilized on lignocellulosic materials under non-sterile conditions. *J. Clean. Prod.* **2021**, *287*, 125037. [[CrossRef](#)]
6. Morya, R.; Raj, T.; Lee, Y.; Pandey, A.K.; Kumar, D.; Singhanian, R.R.; Singh, S.; Verma, J.P.; Kim, S.-H. Recent updates in biohydrogen production strategies and life-cycle assessment for sustainable future. *Bioresour. Technol.* **2022**, *366*, 128159. [[CrossRef](#)]
7. Shah, A.; Favaro, L.; Alibardi, L.; Cagnin, L.; Sardon, A.; Cossu, R.; Casella, S.; Basaglia, M. *Bacillus* sp. strains to produce bio-hydrogen from the organic fraction of municipal solid waste. *Appl. Energy* **2016**, *176*, 116–124. [[CrossRef](#)]

8. Cabrol, L.; Marone, A.; Tapia-Venegas, E.; Steyer, J.-P.; Ruiz-Filippi, G.; Trably, E. Microbial ecology of fermentative hydrogen producing bioprocesses: Useful insights for driving the ecosystem function. *FEMS Microbiol. Rev.* **2017**, *41*, 158–181. [[CrossRef](#)]
9. Guo, X.M.; Trably, E.; Latrille, E.; Carrere, H.; Steyer, J.-P. Hydrogen production from agricultural waste by dark fermentation: A review. *Int. J. Hydrogen Energy* **2010**, *35*, 10660–10673. [[CrossRef](#)]
10. García-Depraect, O.; Castro-Muñoz, R.; Muñoz, R.; Rene, E.R.; León-Becerril, E.; Valdez-Vazquez, I.; Kumar, G.; Reyes-Alvarado, L.C.; Martínez-Mendoza, L.J.; Carrillo-Reyes, J.; et al. A review on the factors influencing biohydrogen production from lactate: The key to unlocking enhanced dark fermentative processes. *Bioresour. Technol.* **2021**, *324*, 124595. [[CrossRef](#)]
11. Sikora, A.; Błaszczak, M.; Jurkowski, M.; Zielenkiewicz, U. Lactic acid bacteria in hydrogen-producing consortia: On purpose or by coincidence? In *Lactic Acid Bacteria—R & D for Food, Health and Livestock Purposes*, 1st ed.; Kongo, J.M., Ed.; InTech: London, UK, 2013.
12. Martínez-Mendoza, L.J.; Lebrero, R.; Muñoz, R.; García-Depraect, O. Influence of key operational parameters on biohydrogen production from fruit and vegetable waste via lactate-driven dark fermentation. *Bioresour. Technol.* **2022**, *364*, 128070. [[CrossRef](#)] [[PubMed](#)]
13. Regueira-Marcos, L.; García-Depraect, O.; Muñoz, R. Elucidating the role of pH and total solids content in the co-production of biohydrogen and carboxylic acids from food waste via lactate-driven dark fermentation. *Fuel* **2023**, *338*, 127238. [[CrossRef](#)]
14. García-Depraect, O.; Rene, E.R.; Diaz-Cruces, V.F.; León-Becerril, E. Effect of process parameters on enhanced biohydrogen production from tequila vinasse via the lactate-acetate pathway. *Bioresour. Technol.* **2019**, *273*, 618–626. [[CrossRef](#)] [[PubMed](#)]
15. García-Depraect, O.; Lebrero, R.; Rodríguez-Vega, S.; Börner, R.A.; Börner, T.; Muñoz, R. Production of volatile fatty acids (VFAs) from five commercial bioplastics via acidogenic fermentation. *Bioresour. Technol.* **2022**, *360*, 127655. [[CrossRef](#)] [[PubMed](#)]
16. Kim, D.-H.; Lim, W.-T.; Lee, M.-K.; Kim, M.-S. Effect of temperature on continuous fermentative lactic acid (LA) production and bacterial community, and development of LA-producing UASB reactor. *Bioresour. Technol.* **2012**, *119*, 355–361. [[CrossRef](#)] [[PubMed](#)]
17. García-Depraect, O.; Gómez-Romero, J.; León-Becerril, E.; López-López, A. A novel biohydrogen production process: Co-digestion of vinasse and *Nejayote* as complex raw substrates using a robust inoculum. *Int. J. Hydrogen Energy* **2017**, *42*, 5820–5831. [[CrossRef](#)]
18. Gomez-Romero, J.; Gonzalez-Garcia, A.; Chairez, I.; Torres, L.; Garcia-Peña, E.I. Selective adaptation of an anaerobic microbial community: Biohydrogen production by co-digestion of cheese whey and vegetables fruit waste. *Int. J. Hydrogen Energy* **2014**, *39*, 12541–12550. [[CrossRef](#)]
19. Tao, Y.; Hu, X.; Zhu, X.; Jin, H.; Xu, Z.; Tang, Q.; Li, X. Production of butyrate from lactate by a newly isolated *Clostridium* sp. BPY5. *Appl. Biochem. Biotechnol.* **2016**, *179*, 361–374. [[CrossRef](#)]
20. Juang, C.-P.; Whang, L.-M.; Cheng, H.-H. Evaluation of bioenergy recovery processes treating organic residues from ethanol fermentation process. *Bioresour. Technol.* **2011**, *102*, 5394–5399. [[CrossRef](#)]
21. Sträuber, H.; Lucas, R.; Kleinstaub, S. Metabolic and microbial community dynamics during the anaerobic digestion of maize silage in a two-phase process. *Appl. Microbiol. Biotechnol.* **2016**, *100*, 479–491. [[CrossRef](#)]
22. Regueira-Marcos, L.; Muñoz, R.; García-Depraect, O. Continuous lactate-driven dark fermentation of restaurant food waste: Process characterization and new insights on transient feast/famine perturbations. *Bioresour. Technol.* **2023**, *385*, 129385. [[CrossRef](#)]
23. García-Depraect, O.; Diaz-Cruces, V.F.; Rene, E.R.; Castro-Muñoz, R.; León-Becerril, E. Long-term preservation of hydrogenogenic biomass by refrigeration: Reactivation characteristics and microbial community structure. *Bioresour. Technol. Rep.* **2020**, *12*, 100587. [[CrossRef](#)]
24. García-Depraect, O.; León-Becerril, E. Fermentative biohydrogen production from tequila vinasse via the lactate-acetate pathway: Operational performance, kinetic analysis and microbial ecology. *Fuel* **2018**, *234*, 151–160. [[CrossRef](#)]
25. De Gioannis, G.; Friargiu, M.; Massi, E.; Muntoni, A.; Poletini, A.; Pomi, R.; Spiga, D. Biohydrogen production from dark fermentation of cheese whey: Influence of pH. *Int. J. Hydrogen Energy* **2014**, *39*, 20930–20941. [[CrossRef](#)]
26. García-Depraect, O.; Rene, E.R.; Gómez-Romero, J.; López-López, A.; León-Becerril, E. Enhanced biohydrogen production from the dark co-fermentation of tequila vinasse and nixtamalization wastewater: Novel insights into ecological regulation by pH. *Fuel* **2019**, *253*, 159–166. [[CrossRef](#)]
27. García-Depraect, O.; Martínez-Mendoza, L.J.; Diaz, I.; Muñoz, R. Two-stage anaerobic digestion of food waste: Enhanced bioenergy production rate by steering lactate-type fermentation during hydrolysis-acidogenesis. *Bioresour. Technol.* **2022**, *358*, 127358. [[CrossRef](#)] [[PubMed](#)]
28. APHA. *Standard Methods for the Examination of Water and Wastewater*, 21st ed.; American Public Health Association: Washington, DC, USA; American Water Works Association: Denver, CO, USA; Water Environment Federation: Alexandria, VA, USA, 2005.
29. García-Depraect, O.; Muñoz, R.; Rodríguez, E.; Rene, E.R.; León-Becerril, E. Microbial ecology of a lactate-driven dark fermentation process producing hydrogen under carbohydrate-limiting conditions. *Int. J. Hydrogen Energy* **2021**, *46*, 11284–11296. [[CrossRef](#)]
30. Asunis, F.; Carucci, A.; De Gioannis, G.; Farru, G.; Muntoni, A.; Poletini, A.; Pomi, R.; Rossi, A.; Spiga, D. Combined biohydrogen and polyhydroxyalkanoates production from sheep cheese whey by a mixed microbial culture. *J. Environ. Manag.* **2022**, *322*, 116149. [[CrossRef](#)]
31. Aranda-Jaramillo, B.; León-Becerril, E.; Aguilar-Juárez, O.; Castro-Muñoz, R.; García-Depraect, O. Feasibility study of biohydrogen production from acid cheese whey via lactate-driven dark fermentation. *Fermentation* **2023**, *9*, 644. [[CrossRef](#)]

32. Martínez-Mendoza, L.J.; García-Depraect, O.; Muñoz, R. Unlocking the high-rate continuous performance of fermentative hydrogen bioproduction from fruit and vegetable residues by modulating hydraulic retention time. *Bioresour. Technol.* **2023**, *373*, 128716. [[CrossRef](#)]
33. Montoya, A.C.V.; da Silva Mazareli, R.C.; Delforno, T.P.; Centurion, V.B.; Sakamoto, I.K.; de Oliveira, V.M.; Silva, E.L.; Varesche, M.B.A. Hydrogen, alcohols and volatile fatty acids from the co-digestion of coffee waste (coffee pulp, husk, and processing wastewater) by applying autochthonous microorganisms. *Int. J. Hydrogen Energy* **2019**, *44*, 21434–21450. [[CrossRef](#)]
34. Blanco, V.M.C.; Oliveira, G.H.D.D.; Zaiat, M. Dark fermentative biohydrogen production from synthetic cheese whey in an anaerobic structured-bed reactor: Performance evaluation and kinetic modeling. *Renew. Energy* **2019**, *139*, 1310–1319. [[CrossRef](#)]
35. Asunis, F.; De Gioannis, G.; Isipato, M.; Muntoni, A.; Poletini, A.; Pomi, R.; Rossi, A.; Spiga, D. Control of fermentation duration and pH to orient biochemicals and biofuels production from cheese whey. *Bioresour. Technol.* **2019**, *289*, 121722. [[CrossRef](#)] [[PubMed](#)]
36. Dareioti, M.A.; Vavouraki, A.I.; Kornaros, M. Effect of pH on the anaerobic acidogenesis of agroindustrial wastewaters for maximization of bio-hydrogen production: A lab-scale evaluation using batch tests. *Bioresour. Technol.* **2014**, *162*, 218–227. [[CrossRef](#)] [[PubMed](#)]
37. Fuess, L.T.; Júnior, A.D.N.F.; Machado, C.B.; Zaiat, M. Temporal dynamics and metabolic correlation between lactate-producing and hydrogen-producing bacteria in sugarcane vinasse dark fermentation: The key role of lactate. *Bioresour. Technol.* **2018**, *247*, 426–433. [[CrossRef](#)]
38. Sivagurunathan, P.; Kumar, G.; Park, J.-H.; Park, J.-H.; Park, H.-D.; Yoon, J.-J.; Kim, S.-H. Feasibility of enriched mixed cultures obtained by repeated batch transfer in continuous hydrogen fermentation. *Int. J. Hydrogen Energy* **2016**, *41*, 4393–4403. [[CrossRef](#)]
39. García-Depraect, O.; Diaz-Cruces, V.F.; Rene, E.R.; León-Becerril, E. Changes in performance and bacterial communities in a continuous biohydrogen-producing reactor subjected to substrate-and pH-induced perturbations. *Bioresour. Technol. Rep.* **2020**, *295*, 122182. [[CrossRef](#)]
40. Hung, C.-H.; Chang, Y.-T.; Chang, Y.-J. Roles of microorganisms other than *Clostridium* and *Enterobacter* in anaerobic fermentative biohydrogen production systems—A review. *Bioresour. Technol.* **2011**, *102*, 8437–8444. [[CrossRef](#)]
41. Ohnishi, A.; Bando, Y.; Fujimoto, N.; Suzuki, M. Development of a simple bio-hydrogen production system through dark fermentation by using unique microflora. *Int. J. Hydrogen Energy* **2010**, *35*, 8544–8553. [[CrossRef](#)]
42. Gadhamshetty, V.; Johnson, D.C.; Nirmalakhandan, N.; Smith, G.B.; Deng, S. Feasibility of biohydrogen production at low temperatures in unbuffered reactors. *Int. J. Hydrogen Energy* **2009**, *34*, 1233–1243. [[CrossRef](#)]
43. Grause, G.; Igarashi, M.; Kameda, T.; Yoshioka, T. Lactic acid as a substrate for fermentative hydrogen production. *Int. J. Hydrogen Energy* **2012**, *37*, 16967–16973. [[CrossRef](#)]
44. Marone, A.; Izzo, G.; Mentuccia, L.; Massini, G.; Paganin, P.; Rosa, S.; Varrone, C.; Signorini, A. Vegetable waste as substrate and source of suitable microflora for bio-hydrogen production. *Renew. Energy* **2014**, *68*, 6–13. [[CrossRef](#)]
45. Kim, D.-H.; Kim, S.-H.; Shin, H.-S. Hydrogen fermentation of food waste without inoculum addition. *Enzym. Microb. Technol.* **2009**, *45*, 181–187. [[CrossRef](#)]
46. He, Y.; Cassarini, C.; Marciano, F.; Lens, P.N. Homoacetogenesis and solventogenesis from H₂/CO₂ by granular sludge at 25, 37 and 55 °C. *Chemosphere* **2021**, *265*, 128649. [[CrossRef](#)]
47. De Vrieze, J.; Verstraete, W. Perspectives for microbial community composition in anaerobic digestion: From abundance and activity to connectivity. *Environ. Microbiol.* **2016**, *18*, 2797–2809. [[CrossRef](#)]
48. Yang, P.; Zhang, R.; McGarvey, J.A.; Benemann, J.R. Biohydrogen production from cheese processing wastewater by anaerobic fermentation using mixed microbial communities. *Int. J. Hydrogen Energy* **2007**, *32*, 4761–4771. [[CrossRef](#)]
49. Sivagurunathan, P.; Sahoo, P.C.; Kumar, M.; Gupta, R.P.; Bhattacharyya, D.; Ramakumar, S.S.V. Unrevealing the role of metal oxide nanoparticles on biohydrogen production by *Lactobacillus delbrueckii*. *Bioresour. Technol.* **2023**, *367*, 128260. [[CrossRef](#)]
50. Castelló, E.; Santos, C.G.; Iglesias, T.; Paolino, G.; Wenzel, J.; Borzacconi, L.; Etchebehere, C. Feasibility of biohydrogen production from cheese whey using a UASB reactor: Links between microbial community and reactor performance. *Int. J. Hydrogen Energy* **2009**, *34*, 5674–5682. [[CrossRef](#)]

Disclaimer/Publisher's Note: The statements, opinions and data contained in all publications are solely those of the individual author(s) and contributor(s) and not of MDPI and/or the editor(s). MDPI and/or the editor(s) disclaim responsibility for any injury to people or property resulting from any ideas, methods, instructions or products referred to in the content.